DQRM: Deep Quantized Recommendation Models

Anonymous Author(s)

ABSTRACT

Large-scale recommendation models are currently the dominant workload for many large Internet companies. These recommenders are characterized by massive embedding tables that are sparsely accessed by index for user and item features. The size of these 1TB+ tables imposes a severe memory bottleneck for recommendation model training and inference. In this work, we propose a novel recommendation framework that is small, powerful, and efficient to train, based on the state-of-the-art Deep Learning Recommendation Model (DLRM). The proposed framework makes inference more efficient on the cloud servers, explores the possibility of deploying powerful recommendations on smaller edge devices, and optimizes the workload of the distributed communication overhead in training under the Data Parallelism settings. Specifically, we show that Quantization-aware Training (QAT) can impose a strong regularization effect to mitigate the severe overfitting issues suffered by DLRMs. Benefiting from the higher efficiency of training data utilization, we achieved uniform INT4 quantization of DLRM models without any accuracy drop. We further propose two techniques that improve and speed up the conventional QAT workload specifically for the embedding tables in the recommendation models. Moreover, distributed training time is dominated by communication overhead. To optimize for the gradient communication, we quantize the gradients of the embedding tables into INT8 on top of the well-supported strong specified sparsification. We show that combining gradient sparsification and quantization together drastically reduces the amount of communication, only incurring a small reasonable accuracy drop. All the code and experiments are open-sourced at: https://anonymous.4open.science/r/Deep_Quantized_Recommendation_Model_DQRM-6B4D

CCS CONCEPTS

• **Computing Systems** → *Efficient Large-scale Neural Network Training*; *Distributed Training*; • **Networks**;

KEYWORDS

Neural Networks, Recommendation Systems, Quantization, Efficiency Distributed Training, Data Parallelism, Regularization

ACM Reference Format:

Anonymous Author(s). 2023. DQRM: Deep Quantized Recommendation Models. In *Proceedings of Make sure to enter the correct conference title from your rights confirmation email (Conference acronym 'XX)*. ACM, New York, NY, USA, 14 pages. https://doi.org/XXXXXXX.XXXXXXX

Conference acronym 'XX, June 03–05, 2018, Woodstock, NY

ACM ISBN 978-1-4503-XXXX-X/18/06…$15.00
https://doi.org/XXXXXXX.XXXXXXX

1 INTRODUCTION

With the widespread adoption of Internet services, personalization becomes a critical function of the services provided by the current Internet giants. Every service users' unique taste and preferences need to be catered to. With billions of Internet users present today, the need for recommendation models is crucial. According to [8], over 79% of the entire Meta's cloud ML inference cycles are spent on the inference of various sizes of recommendation models. By Amdahl's law, a slight boost in recommendation model efficiency can yield a massive performance boost, which can be highly beneficial to large internet companies. On the other hand, if part of the inference workload can be migrated to edge devices, Internet service providers can save precious cloud resources, while the users will have less of their personal data sent to the cloud environment, which strengthens their personal data privacy. Both the company and the end users benefit. In this work, we propose a new recommendation model framework that is small, powerful, and efficient to train. The proposed recommendation models are both more efficient in inference on the cloud environment and possible to fit on edge devices for inference. Also, because of the necessity for periodic retraining in the recommendation models, the proposed framework is optimized for model training in the cloud-distributed environment.

Designing Deep Learning based Recommendation Models is challenging, because of the necessity to both process dense and sparse inputs. Successful previous works [16, 22] utilize massive embedding tables, each corresponding to a sparse feature category. Embedding tables are proven to learn sparse features well. However, embedding tables are usually massive, easily taking up many GB, and in some cases even TB in DRAM memory. The massive model size makes memory the prime bottleneck in both training and inference. The severe memory bottleneck motivates a huge effort in shrinking recommendation model size [3, 6, 7, 13, 15, 20].

In this work, we base our model framework on the Deep Learning Recommendation Model (DLRM) [16], the state-of-the-art recommendation model for Click-Through-Rate (CTR) prediction. The model architecture is summarized in Figure 1 (a). Specifically, we observe that DLRM models can suffer from severe overfitting issues, with testing accuracy dropping steeply after the first one or two epochs of training. We propose to heavily quantize the DLRM model into ultra-low precision INT4 and show that Quantization-aware Training (QAT) imposes a strong regularization effect on DLRM training. When strong quantization is applied, the convergence of the model is initially slower than the full precision model. However, we show QAT is able to improve testing accuracy for more than five epochs (as opposed to overfitting after two epochs) benefiting from the strong regularization effect for overcoming overfitting and higher data efficiency to utilizing precious training data. We achieve comparable testing accuracy with the unquantized model, or even exceed that in some cases, by applying INT4 quantization on the entire model. Our experiments indicate that conventional QAT can be highly inefficient in recommendation model quantization. We

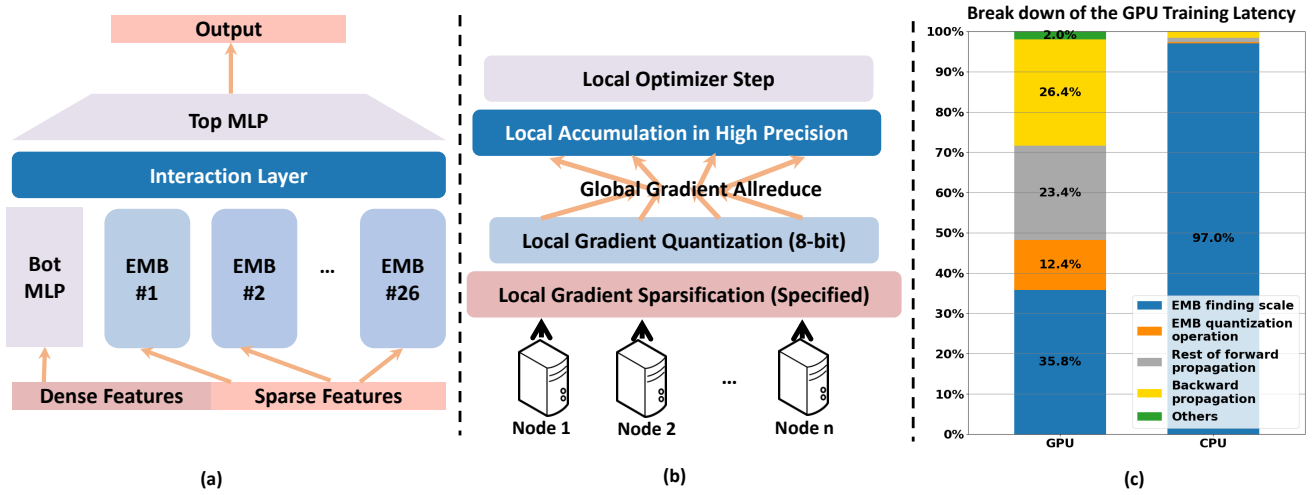

Figure 1: (a) shows the state-of-the-art large-scale recommendation model architecture. The model contains two types of layers: Embedding tables and MLP layers. (b) depicts the entire gradient compression and communication during the training of the DQRM quantization framework. (c) shows a breakdown of the training time on four NVIDIA M40 GPUs running QAT of DLRM with only embedding table quantization; the majority of the training time is spent on finding the quantization scale, and even more so on the CPU clusters. (Figure best viewed in color)

propose two techniques that reduce additional memory copies of large embedding tables during QAT and drastically speed up the training time, which is dominated by the traversal of large tensors in memory to compute the quantization scale parameters.

Training DLRM-like models usually occurs in a highly distributed cloud environment. The training time is usually dominated by heavy inter and intra-node communications overhead. We propose to apply communication sparsification and quantization together to shrink the communication workload occurring in each iteration. Specifically, we target the Data Parallelism environment. We show that using well-supported specified sparsification (embedding table gradients are nonzero only for vectors that are active in the current iteration) of gradients can compress the communication by three orders of magnitude. On top of that, we further quantize the communication messages from the massive embedding tables into INT8, shrinking the remaining size of communication by one-half during training on the large Criteo Terabyte data set. Also, when both sparsification and quantization are added, we show that the accuracy degradation is reasonably small. We summarize and show the entire backpropagation of the proposed framework in Figure 1 (b). In this paper, we call these quantization and sparsity improvements to DLRM - the Deep Quantized Recommendation Model (DQRM).

We summarize the contribution of this work as three-fold:

- Propose a novel recommender system network that is small, powerful, and fast to train,
- Improve the speed of QAT on recommender system models,
- Utilize both sparsification and quantization of gradients on recommender system models.

This paper is organized as follows: Section 2 presents the summary of techniques and features of DQRM. Section 3 presents the detailed experiment settings and results evaluating the DQRM framework on the two public CTR datasets: Criteo Kaggle and Criteo Terabyte datasets, while Section 4 further provides ablation studies which offer in-depth experiments that support features' effectiveness in shrinking the large-scale recommendation model DLRM. Section 5 summarizes the previous related works on model quantization, recommendation model size compression, and efficient recommendation model training, and we conclude the work in Section 6.

2 METHODOLOGY

2.1 Quantization-aware Training

In this work, we utilize uniform symmetric quantization. When quantizing a floating point number x, we calculate a mapping between x and an integer number I between $[-2^{b-1}, 2^{b-1} - 1]$. Formally, quantization is defined as:

$$I = Q(x, k) = \frac{clip(x, -\alpha, \alpha)}{S}$$

where Q is the quantization function and S is the quantization scale. In this work, we use uniform quantization where S is determined using the following formula:

$$S = \frac{\alpha}{2^{b-1} - 1}$$

In both of the above equations, the term α is the clipping range of quantization, usually determined by the minimum and the maximum of the distribution of the model weights, X.

In this work, we directly use $max(abs(max(x)), abs(min(x)))$ to compute the clipping range α. During experimentation, we found that the minimum and the maximum of the embedding weights are constantly growing, widening the range of clipping continuously. A more detailed study can be found in Appendix C.2. Percentile clipping adds additional overhead in embedding table

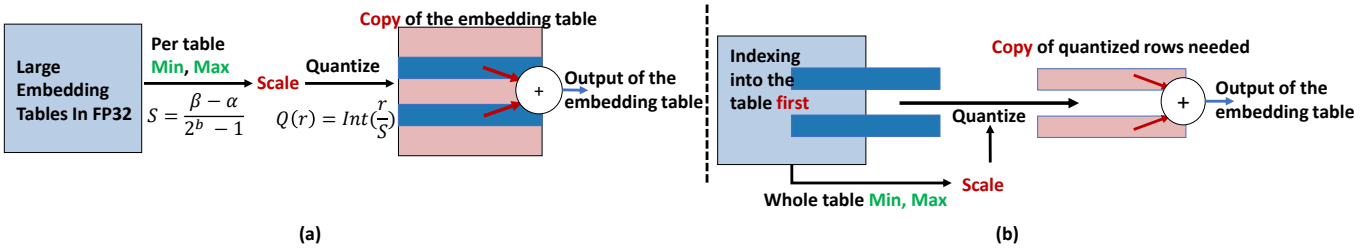

Figure 2: (a) Conventional QAT method, where the entire set of weights of the embeddings are copied and quantized. As embedding accesses are very sparse, this method is wasteful as it processes unused entries and worsens the memory bottleneck in QAT. (b) Our method to avoid the massive copy is by first performing the functional part of each table and then performing copying and quantization. In this way, only part of the weights that are actually used is copied and quantized, utilizing the memory more efficiently. (Figure best viewed in color).

traversal, which, as we show later, is a big challenge for quantizing embedding tables. On the other hand, the trained clipping range may be sub-optimal for the moving target.

We are aware of previous works [7] that use a non-uniform codebook quantization for quantizing embedding tables. Although codebook quantization theoretically can find a better fit for an arbitrary weight distribution, without complex implementation support, it slows down the process of quantization, which is less significant in Post-Training Quantization (PTQ) which their work is based on and more significant in our work which uses Quantization-aware Training (QAT). The quantization used in this work is symmetric, meaning that the minimum of the clipping range is the mirror image of the maximum. During testing or inference of the quantized model, the scale is unchanged and static.

We deploy Quantization-aware Training (QAT) extensively in our framework. A striking difference between QAT and Post-Training Quantization (PTQ) is the retraining process (finetuning) that comes after the initial usual pretraining using full precision and later quantization into low-precision. During every iteration of the finetuning process of the quantized model, a copy of full precision weights is always stored, which is updated by the gradients in the back-propagation. After updating the full precision weights from the previous iteration, the model is quantized again based on the full precision model from the previous iteration. However, when training large-scale DLRM models in particular, having both the quantized and the full precision model copies introduces additional inefficiencies in memory utilization, which Section 2.2 addresses.

2.2 Reducing additional memory of unused weights

Unlike other popular neural network architectures such as CNNs or transformers, embedding tables occupy over 99% of the entire model size for DLRM-style recommenders. From these giant embedding tables, previous works [6, 15] have shown that training large-scale recommendation models is usually memory-bound, instead of compute-bound as in CNNs and transformers. Additionally, we find that when running the conventional QAT workflow on DLRM näively, the existing memory bottleneck is exacerbated even further.

We present a schematic illustrating our quantization approach in Figure 2 (a). Conventionally, all the weight tensors inside convolutional layers or linear layers contribute to the computation in subsequent layers of the model. Therefore, the entire weight tensor in the quantized layer needs to be quantized. As mentioned previously, preserving a copy of full precision weights is required in QAT. Therefore, we now have a full-precision and a low-precision quantized shadow copy of the same tensor. If such a method is näively applied to embedding table quantization. This entire giant embedding table needs to be copied in memory, which is often unnecessary because of the fundamentally different sparse workflow which contrasts that of conventional convolutional and linear layers, where not all the embedding weights contribute to the subsequent stages of computation.

Instead, we propose to selectively run the sparse functional portion of the embedding layer first, indexing into the embedding tables and retrieving the embedding vectors that are actually required in the following layers in the current iteration. Then, only quantize the embedding vectors that are needed. In the backward pass, the gradient can still update the full precision embedding tables. The key is that throughout the entire iteration, only active embedding table entries are copied, and depending on the batch size and the power law distribution within the training dataset, it is usually more than three magnitudes smaller than the number of embedding vectors in the embedding tables on average.

2.3 Periodic Update in Finding Quantization Scale

The giant embedding tables in DLRM-like large-scale recommendation models also pose another big challenge to the conventional quantization workflow. In quantization, the first step is usually finding the quantization scale. Since we use uniform quantization and determine the clipping range for quantization based on embedding table weights on that iteration, we must find the maximum and the minimum value of the entire embedding table during the forward pass of QAT. Given the large embedding table size, this step is very costly.

Shown in Figure 1 (c), we run a breakdown of training time on the distributed Data Parallelism (DP) training of DLRM QAT on four NVIDIA M40 GPUs. To better illustrate the problem, here

we only quantize the embedding tables. Under the DP settings, without adding QAT, distributed DLRM training already consumes 33.05 ms/iter, as shown in the green area bottom in the figure (note-worthily, without communication, the latency falls down to 10* ms/iter). Here, we enable the efficient implementation of QAT for embedding tables presented in Section 2.2 and specified sparsification of the gradient. When QAT is applied, the training time expands to 87.46 ms/iter. We found out that for the heavy training time consumption, nearly half is spent on finding the maximum and minimum of the embedding tables. If the operation of computing quantization scale is left out, the training time drops down to 46.08 ms/iter. In addition, quantization, dequantization, and rounding offers relatively little additional overhead (because only active weights are processed). The breakdown shows that finding an embedding table quantization scale is an important step of designing an efficient quantization framework for DLRM models.

We also run experiments on Intel(R) Xeon(R) Platinum 8280 CPU clusters based on the PyTorch framework. We found that such a problem significantly magnifies on the CPUs. Finding the quantization scale for large DLRM models under the Terabyte dataset settings can take more than 1000 ms per iteration of QAT. The key problem lies in the traversal of extraordinarily large tensors. We show that periodic update of the quantization scale works effectively in solving the huge lag of computing the quantization scale. Periodic updates both amortize the huge quantization overhead to hundreds of iterations without affecting model convergence. We showed no accuracy degradation while amortizing the training latency almost completely on both Kaggle and Terabyte datasets. Detailed experiment settings and results are presented in Section 4.1.

2.4 Distributed training with gradient quantization

With our improved QAT techniques, we can train DLRM-like models in low-precision efficiently. Through our experiments with QAT on DLRM, we find out that, however, when training using low-precision data types, DLRM converges much slower than using standard single-precision floating point. QAT usually requires a few more epochs to converge during training. Also, even though QAT time is significantly reduced compared to the initial unoptimized implementation, it still has additional compute overhead in quantization, taking slightly longer than normal training. To make QAT more efficient and competitive in training time compared with normal training, we further optimize the communication workload that occurs in every iteration.

Although DQRM is able to compress the model size significantly (8X reduction) while maintaining original model accuracy, it converges slower than the unquantized model and takes more epochs to converge. DLRM that are deployed in commercial settings are usually massive and require multi-GPUs or CPU nodes for training. In this work, we focused on the Data Parallelism settings, where communication of gradient occurs every iteration during training. In Figure 3, we profile the total CPU time spent during the entire training process when using the PyTorch built-in specified sparsity on Embedding tables. During the profile, we train DQRM kaggle across four Nvidia A5000 GPUs and DQRM Terabyte across two Intel Xeon Platinum 8280 CPUs. Under the pure Data Parallelism

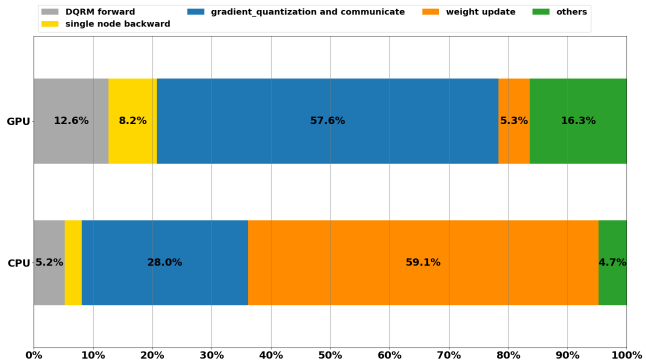

Figure 3: A breakdown of training time on distributed data parallelism environment on multiple GPUs and CPU nodes

settings, gradient communication (blue) is a severe bottleneck for both GPU and CPU platforms. Notice that weight update (orange) portion of CPU platforms is significant, because the vanilla PyTorch library we used is highly inefficient in sparse tensor operations, and the inefficiency in arithmetic will be largely reduced by the recently published IPEX[1] package from Intel. Besides the significant weight update (orange) portion which can be optimized relatively easily, we argue that the gradient communication (blue) is still a severe bottleneck on CPU platform.

Inspired by previous Sparsification [9] and Quantization [23] studies on DLRM models in distributed training message compression, we strive to add gradient quantization on top of heavy gradient sparsification for embedding tables to achieve additional compression ratio. We propose to quantize all gradient into fixed-point INT8 format. However, naively quantizing gradient into INT8 is challenging. Also, naively perform error compensation to all parts of the weights can also be highly inefficient due to the enormous error buffer needed the large embedding tables. Adding large error buffers will drastically increase model size stored into memory during training. In contrary, we identify surprisingly that MLP layers have gradient more sensitive to quantization than embedding tables, and propose to use the Error Compensation technique similar to [23] to reduce accuracy degradation incurred by gradient quantization. We achieve reasonable accuracy degradation while compress the communication message size by roughly 4X on top of the already heavy and well-supported gradient sparsification added to embedding tables. Detailed experiment settings, results, and evaluations are presented in Section 3.3.

3 EXPERIMENT RESULTS

In this section, we present results evaluating the DQRM framework on two commonly used click-through rate recommendation datasets and two DLRM model configurations accordingly. The two datasets are the Criteo Kaggle Display Advertising Challenge Dataset (shortened below as the Kaggle dataset) and the Criteo Terabyte Dataset (shortened as the Terabyte dataset). The original DLRM work [16] proposes two different configurations that are optimized specifically for each dataset, and we followed these two configurations in our implementation of DQRM. We organize the

[1]IPEX official github repo: https://github.com/intel/intel-extension-for-pytorch

results of the experiments under three sections, x.1, x.2, and x.3. Section x.1 details experiments on embedding table quantization alone evaluated on the Kaggle dataset. Section x.2 evaluates DQRM on the Kaggle dataset and on the Terabyte dataset under the distributed settings. Section x.3 evaluates DQRM's effect on communication compression over multiple GPUs and multiple node CPU server environments.

3.1 Quantization of Embedding Tables

Previous works have found that [6, 8] that the embedding tables occupy over 99% of the entire DLRM model size. Therefore, compressing embedding tables is important to the overall DLRM inference model size compression. This section focuses on embedding table quantization, and the experiment results presented in the section are evaluated on the Kaggle Dataset. The specific DLRM model architecture we used is presented in Table 1 under the column labeled Kaggle.

Table 1: DLRM model architecture configurations for Kaggle and Terabyte Datasets

Model Specifications	Kaggle	Terabyte
# Embedding Tables	26	26
Maximum # Row among Tables	10131227	9994101
Embedding Feature Size	16	64
Bottom MLP Arch	13-512-256-64-16	13-512-256-64
Top MLP Arch	512-256-1	512-512-256-1

We used four NVIDIA M40 GPUs to run distributed DQRM Quantization-aware Training (QAT) using a Data Parallel (DP) approach. We deploy uniform fixed-point quantization on the embedding tables. We investigate different bit widths for embedding table quantization: INT16, INT8, INT4, and INT2. Unlike previous works [3, 7] that utilize a per-row based scheme for quantizing embedding tables, for QAT, we quantize the embedding table with a per-table scheme. DLRMs with quantized embedding tables under different settings are all trained for 3 epochs using QAT. Figure 4(a) shows the curves of the testing accuracy during 3 epochs of QAT using different quantization bit widths. The vertical dashed lines signify the boundaries of each epoch. Through our experiments, we found that DLRM in single precision (blue) suffers from severe overfitting after the first epoch, and the testing accuracy drop precipitously afterward. Similarly, when the embedding tables are quantized into INT16 and INT8, the testing accuracies of INT16 (orange) and INT8 (green) quantization follows the same overfitting trend. In contrast, INT4 quantization (red), although it converges slower at the beginning, overcomes overfitting and continues to increase over the entire five epochs. Due to limited space, we don't show the INT2 testing accuracy curve, but its trend is similar to INT4 quantization but it always converges slower with lower accuracy.

We compare the performance after embedding table quantization in Table 2. We extend the QAT training to 5 epochs to let the INT4 and INT2 quantization runs converge further. Although the testing accuracy difference is marginal, a slight increase in accuracy is still considered important for recommendation tasks. Bit widths of INT16 and INT8 lead to comparable performance to the original unquantized DLRM model. Uniform INT4 quantization outperforms the original model in testing accuracy by 0.2% and ROC AUC score by 0.0047. Uniform INT2 quantization leads to a significant accuracy drop (> 0.1% in testing accuracy). From the experiment results, we show that uniform INT4 quantization is capable of preserving the original model accuracy while drastically compressing the original model size with an 8X reduction.

Table 2: DLRM Embedding Tables Quantization, accuracies evaluated on the Kaggle Dataset

Quantization Bit Width	Testing Accuracy	Testing ROC AUC
Unquantized	78.923%	0.8047
INT16	78.772% (+0.043%)	0.8005 (+0.0012)
INT8	78.781% (+0.052%)	0.8007 (+0.0014)
INT4	**78.936% (+0.20%)**	**0.8040 (+0.0047)**
INT2	78.562% (-0.153&)	0.7953 (-0.0040)

3.2 Quantization of the Whole Model

DQRM is based on the well-known DLRM recommender model which contains two major components in its architecture: Embedding Tables and Multi-Layer Perceptrons (MLP). Compared with quantizing only the embedding tables, we observe that MLP layers are much more sensitive to quantization, and implementing this näively can lead to significant accuracy loss, which has been similarly observed in the prior work [3]. We found that using channel-wise quantization of MLP layers is preferred, as it leads to a lower accuracy drop than the full matrix-wise quantization. We evaluate MLP quantization in depth in Section 4.

To better understand the effects of quantization, we evaluate quantizing the whole DLRM model (Embeddings+MLP) into uniform INT4 and tested the performance on both the Kaggle and Terabyte datasets. Following the original DLRM work [16] the specific reference model architectures for the two datasets are different and are summarized in Table 1. The Terabyte reference model is much larger compared to the Kaggle reference model. We used the same experiment platforms for the Kaggle model as in Section 3.1. However, running the Terabyte model is much more resource-demanding. We deploy the models on the Intel Academic Compute Environment (ACE) CPU clusters and specifically use Intel(R) Xeon(R) Platinum 8280 CPUs for model training and inference. The quantized models are all trained using QAT for five epochs. Although we initially found that CPUs can be slower in finding the quantization scale of the embedding tables, a periodic update of the scale can compensate by amortizing the cost of determining the scale during training. This strategy greatly enhances training performance on CPUs. More detailed explanations can be found in the Section 4.1.

We observe similar overfitting issues when training for more than one epoch on the Terabyte dataset, and this concurs with the

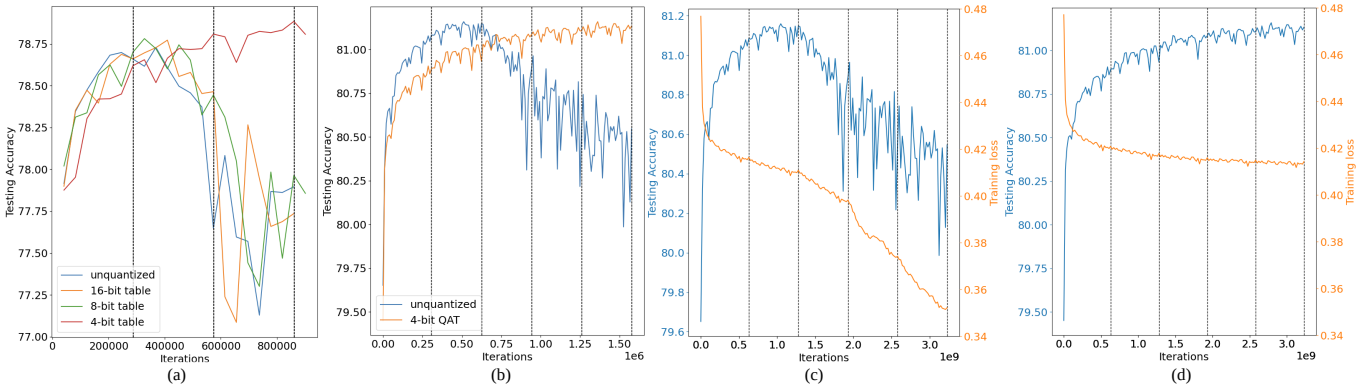

Figure 4: (a) shows the effect of using different QAT bit widths on quantizing embedding tables in DLRM for three epochs of training (epochs are separated by the black dashed lines in all figures). QAT in uniform 4-bit overcomes the severe overfitting suffered by the original DLRM training and leads to significantly higher testing accuracy over three epochs of training. (b) shows the comparison between QAT in 4-bit for DLRM compared to normal training on the Terabyte dataset, and QAT in 4-bit leads to negligible accuracy drop while successfully overcoming the overfitting problem. (c) shows that the training loss (orange curve) for normal training starts decreasing drastically in the third epoch, right where the overfitting occurs. In (d), the training loss curve for QAT in 4-bit decreases stably throughout five epochs of training.

Table 3: DQRM 4-bit quantization results evaluated on Kaggle and Criteo datasets

(a) 4-bit quantization results for DLRM on Kaggle

Quantization Settings	Model Bit Width	Training loss	Testing Accuracy	ROC AUC
Baseline	FP32	0.303685	78.718%	0.8001
Vanilla PTQ	INT4	-	76.571%	0.7675
DQRM	INT4	0.436685	78.897%	0.8035

(b) 4-bit quantization results for DLRM on Criteo

Quantization Settings	Model Bit Width	Training loss	Testing Accuracy	ROC AUC
Baseline	FP32	0.347071	81.165%	0.8004
Vanilla PTQ	INT4	-	78.681%	0.7283
DQRM	INT4	0.409774	81.210%	0.8015

same overfitting seen on the smaller Kaggle dataset. We record the training loss and the testing accuracy curves in Figure 4 (b), (c), and (d). In (b), we contrast the testing accuracies of both original model training and uniform 4-bit QAT. Again, the black vertical dashed lines signify the boundaries of each epoch. At the end of the second epoch, the testing accuracy curve (blue) for the unquantized model drops significantly, while the 4-bit QAT testing accuracy curve (orange) rises steadily and reaches comparable testing accuracies at the end of the fifth epoch. The testing accuracies and the training loss curves are further contrasted for both training scenarios in (c) and (d), unquantized training in (c), and 4-bit QAT in (d). In (c), the training loss curve (orange) for the unquantized model drops drastically at the end of the second epoch, the same time when the model testing accuracy curve (blue) crashes. In contrast, the QAT training loss curve (orange) in (d) decreases steadily throughout the training, while the testing accuracy curve (blue) continues to rise and plateau. In contrast, the 4-bit QAT is effective in regularizing and preventing the severe overfitting issue that normal DLRM model training suffers and is able to utilize the training dataset more effectively.

We report training and testing performance in Table 3. We are aware of the previous Post-Training Quantization (PTQ) efforts [3] for DLRM models. However, previous works neither evaluate the quantized model on the publicly available datasets (Kaggle Terabyte datasets), nor do they publish their implementations. To compare, we showed the testing performance of the vanilla PTQ on quantizing DLRM models in uniform 4-bit. Following the DQRM 4-bit quantization, the vanilla PTQ 4-bit is achieved to have embedding tables quantized channel-wise and MLP quantized row-wise. (a) shows the experimental results on the Kaggle dataset. DQRM is able to get a substantial boost in testing performance while using a significantly smaller bit width INT4 than the unquantized model. DQRM achieves both the higher testing accuracy (78.897%) and the higher testing ROC AUC score (0.8035), which is a more insightful score for binary classification tasks. The boost is conjectured to come from the better behavior DQRM has on heavy overfitting. The vanilla PTQ incurs a significant accuracy drop in both testing accuracy (> 2%) and testing ROC AUC score (> 0.03). (b) presents the experimental results on the Terabyte dataset. DQRM in INT4 incurs an insignificant drop in testing accuracy (0.006%) and testing ROC AUC (0.0006). Similarly, vanilla PTQ in INT4 leads to a significant testing accuracy drop (> 2%), which is suboptimal for quantizing the model.

Table 4: Communications compression for Distributed Data Parallelism training among Four nodes or GPUs

Model Settings	Training Platforms	Communication Compression settings	Communication Overhead per iter	Latency per iter	Training Loss	Testing Accuracy	Testing ROC AUC
Kaggle	4X Nvidia A5000 GPUs	gradient uncompressed (DQRM 4-bit)	2.161 GB	>1000 ms	0.436685	78.897%	0.8035
		+ EMB gradient sparsification (specified)[2]	2.010 MB	61 ms	0.436685	78.897%	0.8035
		+ INT8 gradient Quantization	0.509 MB	110 ms[3]	0.442300	78.840%	0.8023
Terabyte	2X (2 nodes) Intel(R) Xeon(R) Platinum 8280 CPU	gradient uncompressed (DQRM 4-bit)	12.575 GB	>1000 ms	0.412688	81.156%	0.7997
		+ EMB gradient sparsification (specified)	6.756 MB	210 ms	0.412688	81.156%	0.7997
		+ INT8 gradient Quantization	1.732 MB	225 ms	0.414731	81.035%	0.7960

3.3 Gradient Compression

In order to speed up the DQRM training further, communication message reduction is important, and we strive to add gradient quantization on top of the PyTorch-supported heavy sparsification for embedding tables to achieve an additional compression ratio.

In this work specifically, we evaluated the DQRM framework under the synchronous data parallelism settings specifically, where the gradient on all machines allreduced every iteration. We found that the PyTorch `DistributedDataParallel` library doesn't support gradient quantization. In order to experiment on a real distributed environment, we customized our own Data Parallel library on PyTorch that implements gradient quantization locally before the `allreduce` operation. More details of our implementation can be found in Appendix A.1, and we also open-sourced our implementation on the project's official GitHub repository. Our implementation support DP on both multi-GPU and CPU node platform. All gradient compression experiment results are presented in Table 4.

For experiments on the Kaggle dataset, we utilized four NVIDIA A5000 GPUs. Naively, because of the giant model size, when the gradient is completely uncompressed, the overhead of gradient communication is up to 2.1 GB per iteration. Among the overhead, over 99% is from the embedding tables. However, since most rows in the embedding tables are unused in every iteration, the gradients for the unused rows are guaranteed to be zero. PyTorch has built-in support to exploit specified sparsity in the EmbeddingBag modules which can compress 2.1 GB to 2 MB. Also, using specified sparsity is lossless and has no impact on model training performance.

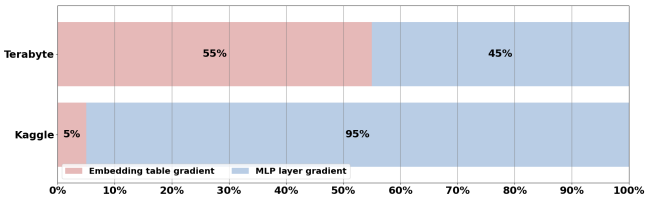

Figure 5: A breakdown of the composition of gradient communication

As shown in section 2.4, heavy embedding gradient sparsification isn't enough alone, as the communication during training continues to bottleneck the training time. On top of the heavily specified sparsity, we add INT8 fixed-point quantization on the gradient to further compress communication size. Interestingly, among the composition of the gradient after sparsification, the MLP gradient occupies a significant portion across both settings. We further add error compensation to the MLP layers only to reduce accuracy degredation. Unfortunately, PyTorch doesn't support low-precision sparse allreduce well. With limited backend support and significant communication overhead caused by sparse tensor coalescing, achieving speedup from communication reduction remains difficult. Currently, local gradient quantization operation per iteration adds additional overhead. We argue that with in-depth system-level optimization for `allreduce` and gradient quantization workload, the training time cost can be further reduced, but such an endeavor is outside the scope of the current work. Nevertheless, we showed that adding gradient quantization only introduces an insignificant decrease 0.057% in the testing accuracy and 0.0012 in the ROC AUC score despite a significant reduction in communication message size.

For experiments on the Terabyte dataset, we ran on two Intel(R) Xeon(R) Platinum 8280 CPU nodes. Similarly, gradient compression of the embedding tables introduces insignificant accuracy loss with roughly 0.1% for testing accuracy and less than 0.004 for testing ROC AUC. We supplement with more evaluations of MLP gradient sensitivity for quantization in the ablation studies.

4 ABLATION STUDIES

In this Section, we present extended studies on the parameters of the DQRM framework, including different update period's impact on DQRM in Section 4.1, different gradient quantization bit width's effect on model convergence in Section 4.2, different sensitivity to quantization among layers in DQRM in Section **??**, and the effect of QAT without retraining on DQRM.

Table 5: Evaluation of Periodic Update on Kaggle and Terabyte Datasets

Model Settings	Period	Latency per iter	Testing Accuracy	Testing ROC AUC
Kaggle	1	71 ms	78.936%	0.8040
	200	46 ms	78.938%	0.8046
	500	46 ms[4]	78.897%	0.8032
Terabyte	1	>1200 ms	-	-
	200	58 ms	81.159%	0.7998
	500	51 ms	81.193%	0.8009
	1000	46 ms	81.210%	0.8015

4.1 Periodic update

Large embedding tables from DQRM models present a unique challenge to normal QAT workflow. As shown in the methodology section, embedding tables are so large that finding the minimum and the maximum element among the table becomes the bottleneck of the forward pass. We propose to utilize periodic updates of the quantization scale of each embedding table during quantization in order to amortize the huge latency of table lookup into multiple iterations. Among the options, we found that the optimal period is different for training settings with different model sizes and batch sizes. The experiment results are presented in Table 5.

Among all the experiments presented in this Section, gradient communication is not quantized. For experiments running on the Kaggle dataset, we run on distributed data parallelism settings using four NVIDIA M40 GPUs. We again trained the model for 5 iterations. Currently, during QAT, only embedding tables are quantized into INT4, while the MLP layers are unquantized and are in FP32. The testing accuracy is expected to be slightly higher than quantizing the whole model as presented previously in section 3.2. On a GPU workload, the training time per iteration decreases significantly, from over 70 ms to 46 ms when the quantization scale is updated once every 200 iterations compared with every iteration. Also, we observed that the model trained does not lose testing performance from 200 iterations of delayed updates for the quantization scale. We also test updating the scale once every 500 iterations, and we observe diminishing gains in training time reduction and a further slight decrease in testing performance.

Similar experiments are conducted on the CPU clusters. We currently use one CPU node to run DQRM under the Terabyte training settings. We found that with the current ML training framework and no additional optimization, CPUs are slower in traversing large embedding tables. A single iteration of training of the model under the Terabyte setting takes more than 1.2 seconds to finish, thus making it impractical to complete the entire training process due to time constraints. Thus, testing performance results are not available. When the quantization scale is periodically updated once every 200 iterations. The training time per iteration drastically improves to 57 ms per iteration. Due to the difference in model size and training mini batch size, we found that using a longer period of 500 iterations brings further speedup in training time per iteration, dropping to 34 ms, while even slightly benefiting the training accuracy (0.03% compared with 200 iterations as the period). We argue that the reason for the slight accuracy boost is that QAT inherently has a quantization scale growing unstably, periodic update of the quantization scale helps stabilize training, which further helps the model converge.

4.2 Different Gradient Quantization Bit Width

In this Section, we present our findings related to the quantization of the gradients during distributed DP training for DQRM. All experiments presented in this Section assume that specified sparsity

[2]specified sparsification is a lossless compression for embedding tables so the testing accuracy is exactly the same as uncompressed case

[3]PyTorch sparse tensor allreduce library doesn't support low-precision arithmetic, without further system level effort in low-precision optimization, the latency per iteration increases purely from the quantization overhead per iteration

[4]rechecking

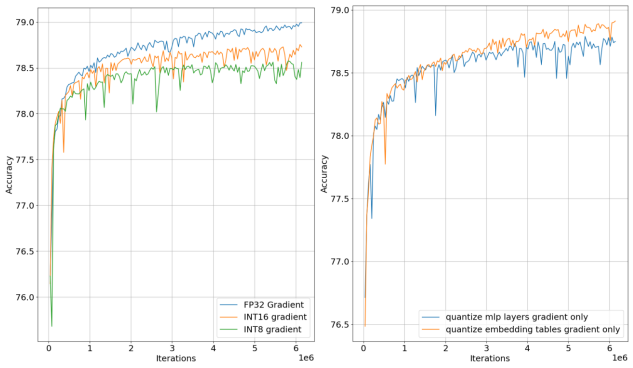

Figure 6: (a) Testing Accuracy of naively quantizing gradients for communication into different bit widths. Naive gradient quantization leads to a significant accuracy drop. (b) MLP gradients are more sensitive to quantization. If only quantizing the embedding table gradients into INT16, it will lead to less drop in accuracy compared to only quantizing MLP gradients into INT16.

is enabled. Firstly, we study the effect of naive quantization of gradients on the model convergence. The experiments are run on a single NVIDIA M40 GPU under a simulated DP environment under Kaggle dataset. More details of the experiment platform setup can be found in Appendix A.2. Quantizing all the gradients naively introduces huge accuracy loss and largely hurts the model convergence. In Figure 6 (a), blue curve signifies the baseline: FP32 gradients. The orange curve is for INT16 gradients, while the green curve is for INT8 quantization gradients. Both the INT16 and the INT8 quantization force the training to plateau earlier and converge to a much lower testing accuracy.

Following our first experiment and setup, we investigate quantizing just embedding table gradients or just MLP layers gradient but not both Figure 6 (b). We show that only quantizing embedding table gradients allows the model to continuously converge throughout the five epochs while quantizing the MLP layers significantly slows down the model convergence. Therefore, we decided to add Error Compensation only to MLP layers' gradients, as MLP layers' gradients are more sensitive to quantization. More experiments are presented in Table 6 on the similar 4 Nvidia A5000 GPUs with our custom framework. We showed that quantizing Embedding Table gradient into INT8 doesn't hurt test accuracy much, and MLP error compensation largely prevents the large accuracy degradation from MLP gradient quantization.

Table 6: Evaluation of MLP Quantization and Error Compensation

Settings	Testing Accuracy	Testing ROC AUC
baseline	78.897%	0.8035
Only Embedding gradient in INT8	78.858%	0.8023
Embedding and MLP gradient in INT8	78.608%	0.7974
Embedding and MLP gradient in INT8 + MLP EC	78.840%	0.8023

4.3 Quantization of Different Part of Models

Table 7: Quantization Evaluation of Each Part of the Model

Settings	Testing Accuracy	Testing ROC AUC
Baseline	78.718%	0.8001
+ Embedding Tables in 4-bit	78.936%	0.8040
+ MLP in 4-bit matrix-wise	78.830%	0.8022
+ MLP in 4-bit channelwise	78.897%	0.8035
+ MLP in 8-bit channelwise	78.950%	0.8045

In DQRM training, we observe that different layers exhibit different sensitivities to quantization. To study this, we utilize four NVIDIA M40 GPUs and conduct experiments on the Kaggle dataset under the distributed DP settings. The experiment results are presented in Table 4.3. Compared with quantizing embedding tables, MLP layers quantization cannot benefit from the diminishing overfitting effect. Instead, when quantizing MLP layers in the matrix-wise fashion into INT4 and quantizing activation during QAT, the DQRM framework fails to converge. When just quantizing the MLP layers in the matrix-wise fashion and without quantizing the activations, DQRM gives more than 0.1% testing accuracy drop, which is a lot for the Kaggle dataset. In contrast, we analyze MLP quantization in the channel-wise fashion, specifically finding a scale for every row inside the linear layer weights. MLP channel-wise quantization outperforms matrix-wise, bringing the overall accuracy loss for the entire INT4 model to be under 0.04% and 0.0005 in testing ROC AUC compared to single precision unquantized MLP model. We also provide the performance of quantizing the MLP layers in INT8 channel-wise, it is on par with the single precision MLP in test accuracy and test ROC AUC score.

4.4 How Quantization Affects Weight Distribution

Here, we strive to provide more intuition of why INT4 quantization can provide stronger resilience towards overfitting. We look into the weight distribution shift of normal unquantized training, the QAT in INT8 training, and the DQRM in INT4. The weight distribution is plotted in Figure 7. The blue histogram displays the distribution of the unquantized weights, while the quantized weights are in orange. More histograms can be found in the Appendix.

The general trend of weight distribution shift during normal DLRM training is to gradually shift outward, which can be noted by the contrast of the blue histogram between (b) the weight distribution after the second epoch and (d) after 5 epochs. We observed that the quantized weights (orange) exhibit a similar outward-shifting trend. DQRM INT4 quantized weights (orange) in (b) and (d) seemingly trace the unquantized weight poorly compared with INT8 weights in (c), having the majority of the weight distributed near the origin while having some portion of the weights located symmetrically around 0. In comparison, (c) shows INT8 can roughly cover the entire weight distribution neatly. We also observe that the FP32 copy of weights under the quantization-aware training regardless of bitwidth are highly similar in distribution compared

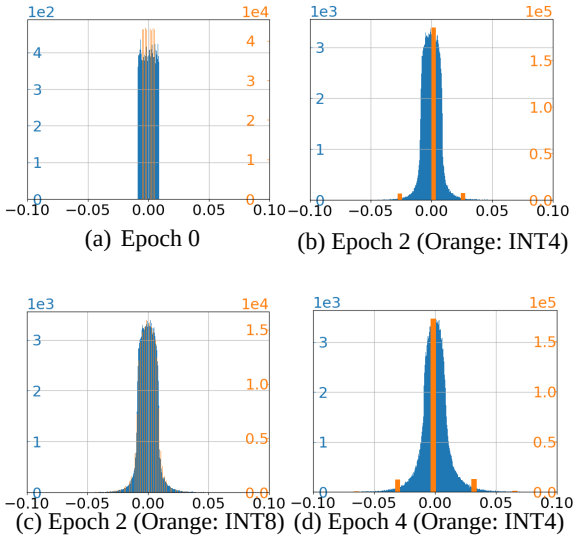

Figure 7: Table 6 in DQRM Kaggle model weight distribution shift. Orange is for the quantized weight distribution under QAT, while blue is for the unquantized weight under normal training. (a) Uniform initialization of embedding tables before training starts. (b) The contrast between unquantized weight and INT4 quantized weight distribution after roughly 2 epochs. (c) Meanwhile, if model is running QAT in INT8 would have different weight distribution (orange) compared with weight during normal training (blue). (d) At the end of 5 epochs of training, DQRM INT4 weight distribution.

with normal training. As shown in section 3.1, INT8 although converges slightly higher than the unquantized model, still follows a similar overfitting trend. We hypothesized that the INT4 quantization resilience towards overfitting comes from its large alienation to normal embedding table weight distribution shift. Also, we observe that the INT4 model has the majority of weights close to zero while performing well, which provokes the thought of whether high sparsity in large embedding tables exists and can be better utilized to tackle overfitting. We leave the question to later works to explore.

5 PREVIOUS WORKS

Neural Network Quantization - Neural network quantization has been widely explored in almost all types of neural networks. We point to one survey paper [5] for a comprehensive summary of quantization development and techniques. Besides, we give some highlights to the most relevant previous works to our project. Quantization-aware Training (QAT) has been widely deployed in CNNs [2, 10–12, 17, 21] and transformers [1, 4, 14, 19, 24]. Compared with Post-Training Quantization (PTQ), QAT benefits from an additional round of fine tuning using low-precision during the forward pass, always achieving lower accuracy loss for various different model architectures. However, because of the extra quantization step, QAT usually takes a much longer time to prepare compared to PTQ. This problem exacerbates in large-scale recommendation models, where conventional QAT worsens the already

severe memory overhead during training, due to the presence of large embedding tables. This work proposes a method to alleviate the issue by optimizing the forward pass of QAT tailored for DLRM-like models.

Compressing Large-scale Recommendation Model - DLRM [16] is the state-of-the-art click-through-rate recommendation model designed and deployed by Meta. However, under the MLPerf settings, the model trained on the Terabyte dataset already contains Embedding tables that require storage of more than 89 GB, which exceeds the memory capacity of every current generation GPU. The giant model size has brought about huge difficulties in both model training and inference, which motivates works that compress the model. Over 99% of the DLRM model size is occupied by the embedding tables, and various previous works attempt to shrink the embedding tables. [6] proposes to shrink the embedding dimension of each embedding table based on their hotness evaluated through a metric based on spectral decay and the popularity of each table. Similarly, [20] proposed to break large embedding tables into smaller sub-tables and combine sub-tables vectors using compositional operations. We argue that both works essentially prune the embedding table sizes and leave the precision of the model unchanged. Our work is complementary to theirs. Also, there are previous works that attempt to quantize the embedding tables and vectors in recommendation models. [13] uses differentiable product quantization for matrix factorization and neural collaborative filtering models, and [15] shows that half-precision quantized model weights benefit the training speed and does not hurt convergence for matrix factorization models. Besides, [7] uses codebook quantization to quantize the embedding tables of DLRM models into INT4 under the PTQ settings, while [3] further quantizes the whole model into 4-bit. Both works revealed that PTQ introduces accuracy degradation which is less competitive with QAT.

Efficient Training of Recommendation Model - On the Matrix Factorization models side, [15] targets model training and proposes to quantize the gradients with dynamic shifting of gradient precision to preserve accuracy. On the other hand, for large-scale recommendation models such as DLRM, the models are usually trained using multiple GPUs or CPU nodes. The training time is heavily affected by the communication strategies between nodes. [9] improved upon conventional Top-k sparsification and applies heavy sparsification to the communication of `all-to-all` and `allreduce` under both Model Parallelism (MP) and Data Parallelism (DP) settings. [23] impose quantization on communication messages under both MP and DP settings and show that with heavy error compensation, the communication workload can be significantly reduced without significant error degradation. On CNN and ASR models, previous work [18] looked at combining sparsification and quantization on communication messages together. However, it shows that the merit of combining the two techniques varies greatly between different layer architectures, making their technique not generalizable to all different model architectures. In this work, we looked into these techniques' effects for different parts of DQRM under the DP environment and combine specified sparsification and quantization together to further benefit DQRM training.

6 CONCLUSION

In this work, we propose a systematic quantization framework DQRM for large-scale recommendation models to make them small, powerful, and efficient to train. Specifically, we discover that the DLRM model suffers severely from the overfitting problem. We show that heavy quantization can help overcome the strong overfitting and utilize the training dataset more efficiently, achieving higher test accuracy eventually. We observe that conventional QAT is troublesome in training large-scale recommendation models and propose two techniques that hugely alleviate the issue. Besides, to further optimize DQRM under the distributed environment, we combine specified sparsification and quantize together to apply to communication gradient compression. Our framework is evaluated intensively on the published dataset, and we provide extensive exploration on detailed feature decision within the DQRM framework.

REFERENCES

[1] Aishwarya Bhandare, Vamsi Sripathi, Deepthi Karkada, Vivek Menon, Sun Choi, Kushal Datta, and Vikram Saletore. 2019. Efficient 8-Bit Quantization of Transformer Neural Machine Language Translation Model. https://doi.org/10.48550/ARXIV.1906.00532

[2] Matthieu Courbariaux, Yoshua Bengio, and Jean-Pierre David. 2015. Binaryconnect: Training deep neural networks with binary weights during propagations. *Advances in neural information processing systems* 28 (2015).

[3] Zhaoxia Deng, Jongsoo Park, Ping Tak Peter Tang, Haixin Liu, Jie Yang, Hector Yuen, Jianyu Huang, Daya Khudia, Xiaohan Wei, Ellie Wen, et al. 2021. Low-precision hardware architectures meet recommendation model inference at scale. *IEEE Micro* 41, 5 (2021), 93–100.

[4] Angela Fan, Edouard Grave, and Armand Joulin. 2019. Reducing transformer depth on demand with structured dropout. *arXiv preprint arXiv:1909.11556* (2019).

[5] Amir Gholami, Sehoon Kim, Zhen Dong, Zhewei Yao, Michael W. Mahoney, and Kurt Keutzer. 2021. A Survey of Quantization Methods for Efficient Neural Network Inference. https://doi.org/10.48550/ARXIV.2103.13630

[6] Antonio A Ginart, Maxim Naumov, Dheevatsa Mudigere, Jiyan Yang, and James Zou. 2021. Mixed dimension embeddings with application to memory-efficient recommendation systems. In *2021 IEEE International Symposium on Information Theory (ISIT)*. IEEE, 2786–2791.

[7] Hui Guan, Andrey Malevich, Jiyan Yang, Jongsoo Park, and Hector Yuen. 2019. Post-training 4-bit quantization on embedding tables. *arXiv preprint arXiv:1911.02079* (2019).

[8] Udit Gupta, Xiaodong Wang, Maxim Naumov, Carole-Jean Wu, Brandon Reagen, David Brooks, Bradford Cottel, Kim M. Hazelwood, Bill Jia, Hsien-Hsin S. Lee, Andrey Malevich, Dheevatsa Mudigere, Mikhail Smelyanskiy, Liang Xiong, and Xuan Zhang. 2019. The Architectural Implications of Facebook's DNN-based Personalized Recommendation. *CoRR* abs/1906.03109 (2019). https://arxiv.org/abs/1906.03109

[9] Vipul Gupta, Dhruv Choudhary, Peter Tang, Xiaohan Wei, Xing Wang, Yuzhen Huang, Arun Kejariwal, Kannan Ramchandran, and Michael W Mahoney. 2021. Training recommender systems at scale: Communication-efficient model and data parallelism. In *Proceedings of the 27th ACM SIGKDD Conference on Knowledge Discovery & Data Mining*. 2928–2936.

[10] Philipp Gysel, Mohammad Motamedi, and Soheil Ghiasi. 2016. Hardware-oriented approximation of convolutional neural networks. *arXiv preprint arXiv:1604.03168* (2016).

[11] Philipp Gysel, Jon Pimentel, Mohammad Motamedi, and Soheil Ghiasi. 2018. Ristretto: A framework for empirical study of resource-efficient inference in convolutional neural networks. *IEEE transactions on neural networks and learning systems* 29, 11 (2018), 5784–5789.

[12] Itay Hubara, Matthieu Courbariaux, Daniel Soudry, Ran El-Yaniv, and Yoshua Bengio. 2016. Binarized neural networks. *Advances in neural information processing systems* 29 (2016).

[13] Wang-Cheng Kang, Derek Zhiyuan Cheng, Ting Chen, Xinyang Yi, Dong Lin, Lichan Hong, and Ed H Chi. 2020. Learning multi-granular quantized embeddings for large-vocab categorical features in recommender systems. In *Companion Proceedings of the Web Conference 2020*. 562–566.

[14] Sehoon Kim, Amir Gholami, Zhewei Yao, Michael W Mahoney, and Kurt Keutzer. 2021. I-bert: Integer-only bert quantization. In *International conference on machine learning*. PMLR, 5506–5518.

[15] Yunyong Ko, Jae-Seo Yu, Hong-Kyun Bae, Yongjun Park, Dongwon Lee, and Sang-Wook Kim. 2021. MASCOT: A Quantization Framework for Efficient Matrix Factorization in Recommender Systems. In *2021 IEEE International Conference on Data Mining (ICDM)*. IEEE, 290–299.

[16] Maxim Naumov, Dheevatsa Mudigere, Hao-Jun Michael Shi, Jianyu Huang, Narayanan Sundaraman, Jongsoo Park, Xiaodong Wang, Udit Gupta, Carole-Jean Wu, Alisson G. Azzolini, Dmytro Dzhulgakov, Andrey Mallevich, Ilia Cherniavskii, Yinghai Lu, Raghuraman Krishnamoorthi, Ansha Yu, Volodymyr Kondratenko, Stephanie Pereira, Xianjie Chen, Wenlin Chen, Vijay Rao, Bill Jia, Liang Xiong, and Misha Smelyanskiy. 2019. Deep Learning Recommendation Model for Personalization and Recommendation Systems. *CoRR* abs/1906.00091 (2019). https://arxiv.org/abs/1906.00091

[17] Renkun Ni, Hong-min Chu, Oscar Castañeda, Ping-yeh Chiang, Christoph Studer, and Tom Goldstein. 2020. WrapNet: Neural Net Inference with Ultra-Low-Resolution Arithmetic. https://doi.org/10.48550/ARXIV.2007.13242

[18] Cedric Renggli, Saleh Ashkboos, Mehdi Aghagolzadeh, Dan Alistarh, and Torsten Hoefler. 2018. SparCML: High-Performance Sparse Communication for Machine Learning. https://doi.org/10.48550/ARXIV.1802.08021

[19] Sheng Shen, Zhen Dong, Jiayu Ye, Linjian Ma, Zhewei Yao, Amir Gholami, Michael W. Mahoney, and Kurt Keutzer. 2019. Q-BERT: Hessian Based Ultra Low Precision Quantization of BERT. (2019). https://doi.org/10.48550/ARXIV.1909.05840

[20] Hao-Jun Michael Shi, Dheevatsa Mudigere, Maxim Naumov, and Jiyan Yang. 2020. Compositional embeddings using complementary partitions for memory-efficient recommendation systems. In *Proceedings of the 26th ACM SIGKDD International Conference on Knowledge Discovery & Data Mining*. 165–175.

[21] Shyam A. Tailor, Javier Fernandez-Marques, and Nicholas D. Lane. 2020. Degree-Quant: Quantization-Aware Training for Graph Neural Networks. https://doi.org/10.48550/ARXIV.2008.05000

[22] Ruoxi Wang, Bin Fu, Gang Fu, and Mingliang Wang. 2017. Deep & cross network for ad click predictions. In *Proceedings of the ADKDD'17*. 1–7.

[23] Jie Amy Yang, Jongsoo Park, Srinivas Sridharan, and Ping Tak Peter Tang. 2020. Training deep learning recommendation model with quantized collective communications. In *Conference on Knowledge Discovery and Data Mining (KDD)*.

[24] Ali Hadi Zadeh, Isak Edo, Omar Mohamed Awad, and Andreas Moshovos. 2020. GOBO: Quantizing Attention-Based NLP Models for Low Latency and Energy Efficient Inference. In *2020 53rd Annual IEEE/ACM International Symposium on Microarchitecture (MICRO)*. IEEE. https://doi.org/10.1109/micro50266.2020.00071

A EXPERIMENT PLATFORMS

A.1 Distributed Environment with Gradient Quantization

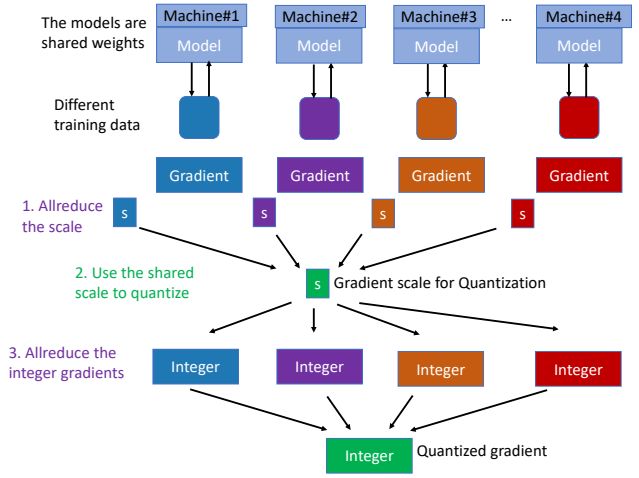

Figure 8: Illustration of the Customized Data Parallelism Framework that Supports Gradient Quantization

In PyTorch DistributedDataParallelism library, during backward propagation, the error tensor's backward() function handles both backpropagating gradients to local parameters together with the all reduce of gradient tensor across nodes. Therefore, after the powerful single line of code, gradients behind each parameter tensor in the distributed data parallelism model have its corresponding gradient ready. However, the quantization of the gradient has to happen between the local backpropagation and the global allreduce. Therefore, distributed data parallelism package is not very handy.

In order to implement gradient quantization, we implement a stand-alone framework that performs the majority of distributed data parallelism workflow. To implement gradient quantization, we summarized our implementation in Figure 8. We start by partitioning the training batch into pieces to be used by different machines. After forward propagation, the local devices are asked to backpropagate the corresponding gradient locally. Then, for all parameters in the model, the following sequence of steps is performed. The quantization scale of parameter tensors is computed locally at first. Computing the quantization scale is completely determined by the quantization bitwidth and local tensor distribution so can be performed locally. Then, the quantization scale is first allreduced to be unified. Then, using the same scale, gradient tensors on each device are quantized locally. The integer gradients are then allreduced. After two all reduce steps, each device then has the same quantization scale and the same quantized gradients. The local step update of parameters then can be dequantized. The quantization bit width used is INT8 and unified across all parameters. When it comes to sparse gradients from embedding tables, we only quantize the `values` part of the `sparse_coo` tensor format and leave the `indices` and other fields unchanged.

One caveat of the entire flow of our customized gradient communication is that it can only be used for allreduce paradigms that perform the reduce operation at the destined machine, such as Ring allreduce. However, for recursive doubling allreduce, where the reduce operation is collectively performed by many machines, our framework is not applicable. The main problem is at each reduce operation, where a sum is taken by two low-precision operations. To continue propagating the gradients under the low-precision bitwidth, an additional rounding should occur, which may potentially lose the gradient precision further. Unfortunately, PyTorch allreduce operations use recursive-doubling allreduce, thoughout our presented experiment, we use FP32 tensors to contain quantized INT8 integer gradients to avoid accumulation and rounding issues from the impact of allreduce.

A.2 Simulated Data Parallelism Environment

Algorithm 1: Simulated Data Parallelism on single machine

```
buffer_clean ← False;
for j, batch in enumerate(train_loader) do
    Z ← model_forward(training_input);
    E ← loss_criterion(Z, label);
    clear_gradient(model);
    if buffer_clean then
        grad_buffer_zero();
        buffer_clean ← False;
    end
    E.backward() ;  /* local backward propagation */
    grad_buffer_update();
    if j % simulated_nodes == 0 then
        weight_buffer_update();
        buffer_clean ← True;
    end
end
```

For some experiments presented in the main content, we use a simulated environment to run Data Parallelism on single device to imitate the multiple device environment. Here we provide more details of our implementation. In our implementation, we add an addition gradient buffer for every parameter tensor. As summarized in 1, the batch size is splited similar to one distributed machine. In the second if statement, the weight is actually updated by the gradient every simulated_node iterations. Between updates, training still backpropagate gradients from relevant iteration and are hold inside the parameter buffers. After weight being updated by the buffer, the buffer is cleared prior to new gradient being backpropagated. One key difference between simulated and the real distributed environment lays in its allreduce mechanism. Shown in section A.1, if gradients are quantized, two allreduce processes occur in one iteration: the first communicates quantization scale, while the second one communicates quantized gradient tensors. However, two allreduce processes are difficult to implement in the simulated environment. Therefore, we reuse the quantization scale of the first iteration throughout simulated_machine number of iterations in our implementation, which can potentially hurts the

gradient quantization precision. However, through our experiments, we didn't observe this case.

A.3 Simulated framework evaluation

Table 8: Multi-node Experiment Results with 8-bit gradients, loss evaluated on the Terabyte Dataset

#Node	Training Loss Drop	Testing Acc Drop	Testing AUC Drop
2	**-0.002447**	0.092	**0.0025**
4	-0.00273	0.114	0.0036
8	-0.00395	**0.059**	0.0053

We also evaluate the effect of different node counts on gradient quantization. The result is listed in Table 8. Currently, different node counts are simulated on the single CPU node. Across three different node counts, 2, 4, and 8, the drop in training loss, testing accuracy, and ROC AUC score are consistent and small.

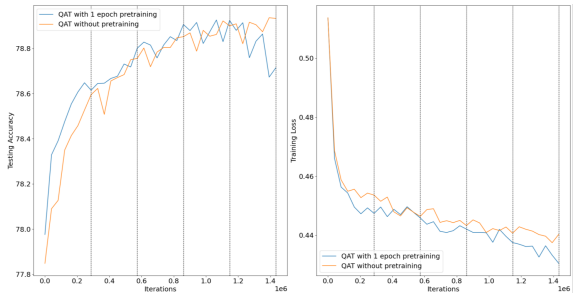

(a) (b)

Figure 9: (a) Testing accuracy over the 5 epochs for 1 epoch of pretraining before 4 epochs of QAT and 5 epochs of QAT without pretraining. Pretraining leads to faster overfitting, and QAT without pretraining avoids overfitting and achieves better testing accuracy from 5 epochs of training. (b) Training loss over the 5 epochs. Pretraining before QAT leads to a faster decrease in training loss in DLRM compared with QAT without pretraining.

B QAT WITHOUT PRE-TRAINING

Table 9: Evaluation of QAT from scratch on Recommendation Models

Settings	Testing Accuracy	Testing ROC AUC
One epoch pretraining + Four epochs of QAT	78.926%	0.8039
Five epochs of QAT without pretraining	78.936%	0.8040

Previously, QAT has always been used as a fine-tuning technique for training CNN and transformer models. Usually, with pretraining on the single-precision bit-width, the trained weights can reduce accuracy loss when fine tuning on low-precision settings. We examine such paradigm on the DLRM models. We train DLRM in QAT but only quantize the embedding tables into INT4 under the Kaggle dataset using four NVIDIA M40 GPUs under the distributed DP settings. We compare DLRM with one epoch of pretraining in the single precision followed by four epochs of INT4 QAT with DLRM with INT4 QAT from scratch.

We plot the testing accuracy versus iteration curves in Figure 6 (a). The experiment results are presented in Table B. In the diagram, the vertical dashed lines signify the boundary of each epoch. The blue curve is for QAT with pretraining, while the orange curve is without. After the first epoch, we can see that as the model transitions from single-precision to INT4 quantized data type, the blue curve drops slightly, which is expected. Further, in the mid third epoch, QAT with pretraining (blue) reaches its peak and then drops quickly afterward. QAT from scratch eventually has a slight testing accuracy edge over QAT with pretraining. Also, in Figure 6 (b), we plot the training loss across five epochs for two different settings. QAT with pretraining (blue) has training loss constantly below QAT from scratch. From here, we argue that QAT with pretraining on DLRM models does speed up the model convergence, taking less number of epochs to reach its peak. However, it suffers from earlier overfitting compared with QAT from scratch. Under our settings, we observe that QAT from scratch slightly gains in testing accuracy of 0.01% with 0.0001 of testing ROC AUC score.

C WEIGHT DISTRIBUTION SHIFT

We provide weight distribution shift with more granularity. Since the experiments performed are separated but of identical experimental settings from the one in section 4.4. The distribution presented in this section will be highly similar, but there might be some minor difference in details.

We select table 6 because table 6 is a medium size embedding table. We found that large tables usually have majority of weights distributed around 0. However, we found that the medium size embedding tables have similar trend with large embedding tables. The model gradually shifted outwards from uniform distribution probability mass function into a bell-shaped curve. Large embedding table has trend similar to that, but still after a few epochs, the majority of weight still gather around 0.

Received 20 February 2007; revised 12 March 2009; accepted 5 June 2009

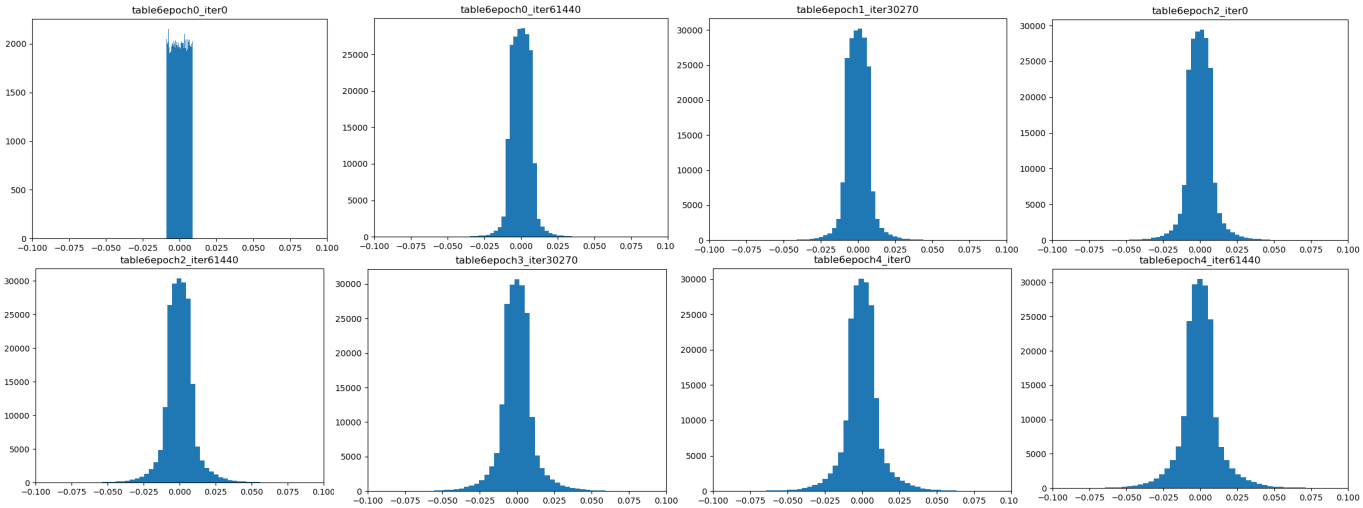

Figure 10: The unquantized weight distribution shift across five epochs. The unquantized model starts overfit after the first epoch

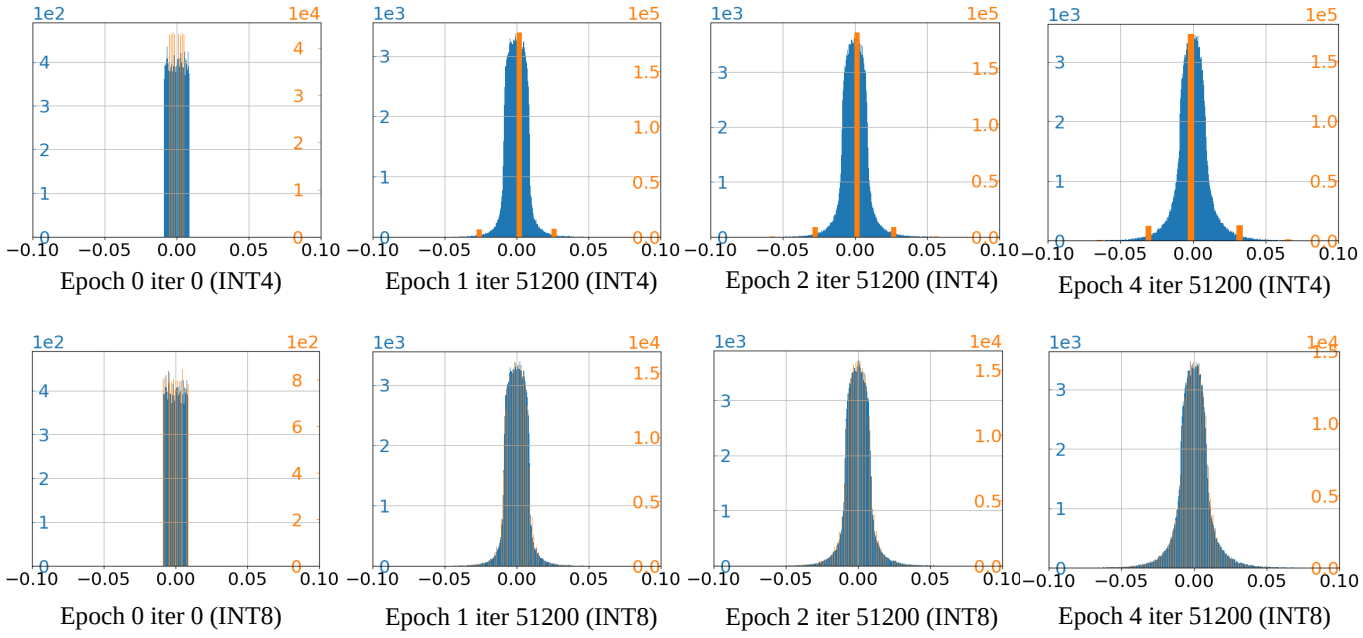

Figure 11: Contrast between INT4 and INT8 quantization-aware training weight distribution shift